

Comparative Study of Various Formulations of Evaporation from Bare Soil Using In Situ Data

J. F. MAHFOUF AND J. NOILHAN

Météo-France/CNRM, 31057 Toulouse, France

(Manuscript received 17 October 1990, in final form 11 February 1991)

ABSTRACT

Various formulations of surface evaporation are tested against in situ data collected over a plot of loamy bare ground. Numerical simulations lasting seven days are compared with observations of near-surface water content and cumulative evaporation.

A comparison of classical bulk aerodynamic formulations shows similar predictions of daytime evaporation while significant differences are exhibited during the night. The so-called "surface moisture availability method" seems to overestimate the nocturnal evaporation flux.

In the context of this dataset, threshold methods strongly underestimate surface evaporation during the whole period of observations. A sensitivity analysis reveals that threshold evaporation (maximum sustainable water flux) is highly sensitive upon the depth of the top soil layer.

1. Introduction

Evaporation over bare ground involves very complex mechanisms since water in soil is not freely available. Exchanges of water vapor between the surface and the atmosphere depend not only on hydraulic transfers within the deep soil but also on the diffusion of water in a thin layer close to the surface where vaporization of soil water takes place. Because of the high nonlinearity of the hydraulic properties of soils (see Mahrt and Pan 1984 for a review), numerical simulation of mass and heat exchanges at the interface requires very detailed models using a high vertical resolution close to the interface (about 1 mm) in order to ensure the continuity of water fluxes at the soil-atmosphere boundary (Sasamori 1970; McCumber and Pielke 1981; Camillo et al. 1983; Passerat et al. 1989). Such models are not suitable for use within meteorological models because they need both a very short time step (namely of the order of 1 min) and large memory storage.

Consequently, simpler parameterizations are required making use of a single prognostic equation for the near-surface water content w_g and an explicit formulation of the evaporation flux E_g . The major difficulty then is to establish a relationship between evaporation and soil moisture. Numerous formulations have been proposed. They can be divided in two main categories. The bulk aerodynamic methods pro-

vide an explicit relation between E_g and w_g by using a parameterization of the surface specific humidity. Such formulas have been examined by Nappo (1975) and Kondo et al. (1990). The second method is based upon the concept of water supply and demand. Evaporation takes place either at a potential rate (atmospheric demand) or at the maximum sustainable water flux at the soil surface (soil supply) when the soil is dry enough (Wetzel and Chang 1987, 1988; Mahrt and Pan 1984; Dickinson 1984). In the second approach, specification of surface specific humidity is not required, but considerable information concerning hydraulic properties in a thin layer is needed, making them very sensitive to the averaging depth to which the near-surface water content is known or predicted by a simple land surface scheme. All these formulations have to be compared with in situ data at the local scales prior to implementation in meteorological models.

In this paper, we use a complete dataset of bare-soil water transfers collected at Monfavet (France) and described in Passerat (1986) and Passerat et al. (1989), to compare the most widely used formulations of surface evaporation. This dataset is very suitable for such a comparison since observations both in the soil and the atmosphere were made continuously during one week, involving significant changes of the near-surface water content from field capacity to dry conditions. Moreover, a detailed model (Passerat 1986) has been calibrated with this dataset, providing a reference for simpler methods. For this study, the near-surface soil water content w_g is computed by the simple parameterization of Noilhan and Planton (1989) (hereafter NP89) derived from the well-known force-restore

Corresponding author address: Dr. Joel Noilhan, Centre National de Recherche Meteorologique, 42, Avenue G. Coriolis, 31057 Toulouse Cedex, France.

method of Deardorff (1977). Another point of interest for us is that, since the NP89 scheme has been widely validated over vegetated surfaces (NP89; Mahfouf and Jacquemin 1989; Mahfouf 1990; Jacquemin and Noilhan 1990; Germain 1990), this work constitutes a complementary investigation over bare ground.

2. An overview of evaporation parameterizations

As shown in Fig. 1, free water in an unsaturated soil is mainly retained in the smaller pores of the soil matrix. Just above the menisci of the free water in the capillarity tubes formed by the soil pores, water vapor is in equilibrium with the liquid phase. Therefore, the air humidity near the surface of water is lower than saturation vapor pressure in a flat free-water surface. From thermodynamic reasoning, the relative humidity h of the air adjacent to the water can be expressed as (Philip 1957):

$$h = \exp(g\psi/R_vT) \tag{1}$$

where g is the acceleration due to gravity, R_v the gas constant of water vapor at temperature T , and ψ the capillarity potential, usually expressed as the height of a water column. This water pressure represents the work needed to bring molecules of water from a unit

mass of soil to the air against surface tension forces between soil and water. Equation (1) provides a convenient relation to express the continuity of mass transfers from the soil to the atmosphere and has been used in detailed water transfer models (Sasamori 1970; McCumber and Pielke 1981; Camillo et al. 1983; Brunet 1984; Mahfouf 1986; Noilhan 1987; Passerat et al. 1989). The computation of h requires a high vertical resolution close to the surface since the gradients of water potential and temperature may be extremely important in this zone, even on the top few millimeters of the soil. Unfortunately, simpler parameterizations generally deal with a single equation for the volumetric water content w_g of a thin layer of a few centimeters as depicted in Fig. 1.

The evaporation of the free water from the soil pores involves two main physical processes:

- (i) molecular diffusion from the water surface to the land surface level, defined as the humidity roughness height Z_{oq} ;
- (ii) laminar and turbulent exchanges from the land surface to the atmosphere.

Prior to summarizing the different ways to parameterize the evaporation, let us define some characteristic quantities:

- the air specific humidity q_a in the atmospheric reference level Z_a ($Z_a \approx 2$ m);
- the surface specific humidity q_g at the roughness height Z_{oq} (see Brutsaert 1982, chapter 5 for a review of Z_{oq} formulations); and
- the specific humidity q_s in the vicinity of the free water in the soil.

Exchanges between the surface and the atmosphere are controlled by the aerodynamic resistance $R_a = (C_E U_a)^{-1}$ where C_E is the drag coefficient for evaporation and U_a the wind speed at Z_a . The coefficient C_E depends on the thermal stability of the lower atmosphere (Louis et al. 1981).

Within the soil, molecular diffusion of water vapor is described by the resistance to the water diffusion R_{soil} in the large soil pores. Choudhury and Monteith (1988) provide a comprehensive description of R_{soil} for a dry soil layer of a few millimeters near the land surface. This quantity is inversely proportional to the molecular diffusivity of vapor (Kondo et al. 1990) and thus is strongly dependent upon both the soil texture and structure. Various empirical formulations of R_{soil} versus soil moisture have been established from in situ data (Table 1). Work has to be done on determining R_{soil} for various soil textures in order to use it in meteorological models.

The classical bulk aerodynamic formulation of E_g follows from the conceptual scheme of Fig. 1. Two distinct methods are usually used. In the so-called α method, E_g is expressed between the levels Z_{oq} and Z_a through:

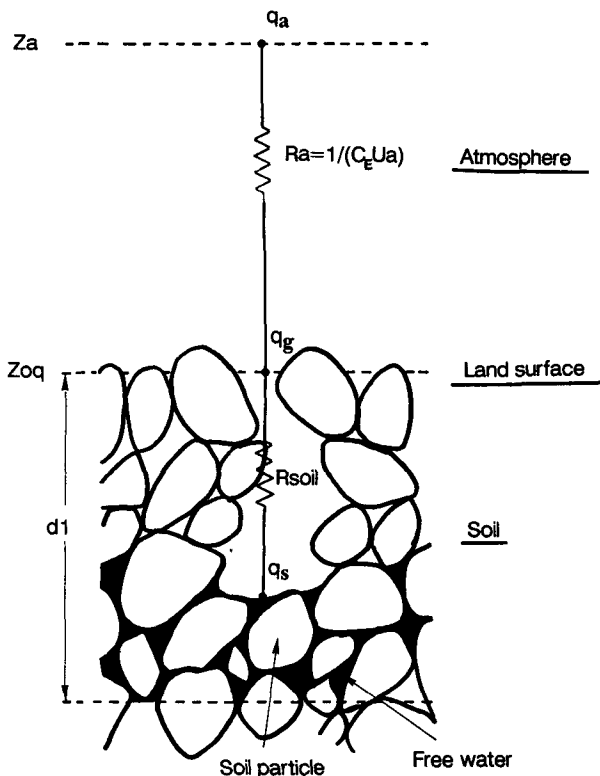


FIG. 1. A schematic description of a surface layer of depth d_1 as proposed by Kondo et al. (1990). Water vapor is diffused through the large pore from the free-water surface to the land surface.

TABLE 1. Methods for calculating E_g : w_{wilt} , w_{fc} and w_{sat} are the volumetric water content at the wilting point, field capacity, and saturation, respectively. The molecular diffusion D_m is given by Eq. (6) from Kondo et al. (1990). The coefficients D and K are the near-surface hydraulic diffusivity and conductivity, respectively. An average soil diffusivity \bar{D} is defined by Eq. (4b) of Dickinson (1984). The coefficient C_K is given by Eq. (4) of Dickinson (1984) and d , d_1 , and d_2 are the depth at which the diurnal cycle of soil moisture is damped, the depth of the top soil layer, and the depth of the total active layer, respectively. The coefficients B and b are textural dependent parameters expressed by Eq. (7) of Wetzal and Chang (1987) and Clapp and Hornberger (1978), respectively.

Bulk aerodynamic formulation		Threshold formulation
$\frac{\rho}{R_a} [\alpha q_{\text{sat}}(T_s) - q_a]$	$\frac{\rho}{R_a} \beta [h q_{\text{sat}}(T_s) - q_a]$	$\min \left\{ \rho_w E_t, \frac{\rho}{R_a} [q_{\text{sat}}(T_s) - q_a] \right\}$
$\alpha = \min \left(1, \frac{1.8 w_g}{w_g + 0.30} \right)$ (B79) (Barton 1979)	$\beta = \min \left(1, \frac{w_g}{0.75 w_{\text{sat}}} \right)$ $h = 1$ (D78) (Deardorff 1978)	$E_t = 2D \frac{w_g - w_{\text{wilt}}}{d_1} - K$ (MP84) (Mahrt and Pan 1984)
$\alpha = \min \left(1, \frac{1.8 w_g}{0.7 w_g + 0.40} \right)$ (YT81) (Yasuda and Toya 1981)	$\beta = \frac{R_a}{R_a + R_{\text{soil}}}$ $h = 1$ $R_{\text{soil}} = 3.5 \left(\frac{w_{\text{sat}}}{w_g} \right)^{2.3} + 33.5$ (S82) (Sun 1982)	$E_t = C_K \bar{D} \frac{w_2}{w_{\text{sat}} \sqrt{d_1 d_2}}$ (D84) (Dickinson 1984)
$\alpha = \frac{1}{2} \left[1 - \cos \left(\frac{w_g \pi}{w_{fc} 2} \right) \right]$ if $w_g < w_{fc}$ $\alpha = 1$ if $w_g \geq w_{fc}$ (NP89) (Noilhan and Planton 1989)	$R_{\text{soil}} = 3.8113 \times 10^4 \exp \left(-13.515 \frac{w_g}{w_{fc}} \right)$ (P86) (Passerat 1986) $R_{\text{soil}} = 216(w_{\text{sat}} - w_g)^{10} / D_m$ (K90) (Kondo et al. 1990) $R_{\text{soil}} = 4140(w_{\text{sat}} - w_g) - 805$ (CG86) $h = \text{Eq. (1)}$ (Camillo and Gurney 1986) (Dorman and Sellers 1989)	$E_t = \frac{B}{\Delta W} \{ w_2^{b+4} - w_{\text{wilt}}^{b+3} [w_2(b+4) - w_{\text{wilt}}(b+3)] \}$ $\Delta W = -d(w_g - w_2)$ (WC87) (Wetzal and Chang 1987) $E_t = \frac{D w_g \pi^2}{4 d_1^2}$ (A88) (Abramopoulos et al. 1988)

$$E_g = \frac{\rho}{R_a} (q_g - q_a) \tag{2}$$

and

$$q_g = \alpha q_{\text{sat}}(T_s), \tag{3}$$

where $q_{\text{sat}}(T_s)$ is the saturated specific humidity at the surface temperature T_s defined as the solution of the surface energy balance. The coefficient α represents the relative humidity of air at the land surface. It has been parameterized as a function of the near-surface water content w_g (Table 1) and most often starts to decrease below the field capacity w_{fc} defined in NP89 as the water content corresponding to an hydraulic conductivity of 0.1 mm day^{-1} .

In the β method, the whole process of evaporation is described from the water level to the atmosphere:

$$E_g = \frac{\rho}{R_a + R_{\text{soil}}} (q_s - q_a) \tag{4}$$

or

$$E_g = \rho C_E U_a \beta (q_s - q_a) \tag{5}$$

and

$$\beta = \frac{1}{1 + C_E U_a R_{\text{soil}}} \tag{6}$$

Table 1 summarizes some expressions for the moisture availability parameter β . One may note the simpler formulation of Deardorff (1977, 1978) depending only on w_g . The specific humidity q_s is given by:

$$q_s = h q_{\text{sat}}(T_s). \tag{7}$$

In Eq. (7), T_s is assumed to be the liquid-vapor interface temperature level but is often computed from the surface energy budget. This tends to overestimate E_g even if the dry superficial layer is extremely thin. This effect is probably reinforced by the fact that several authors set $h = 1$ instead of using Eq. (1). From Table 1, the most complete β methods seems to be that of Camillo and Gurney (1986) and Dorman and Sellers (1989). However, this method requires some knowledge of the relationship between ψ and w_g in the surface relative humidity expression [Eq. (1)] and some reliable parameterization of R_{soil} for a broad range of soil textures.

In the threshold formulation method, evaporation proceeds at the potential rate E_{pot} until the soil moisture supply is sufficiently depleted. Then, E_g is determined by the water flux E_t from below. As a consequence, the evaporation reads:

$$E_g = \min(E_t, E_{\text{pot}}). \tag{8}$$

Table 1 exhibits very different formulations of E_t . All these threshold methods consist in estimating the water flux over a thin layer of depth d . The Mahrt and Pan (1984) expression corresponds to the discretization of the basic transport of water for dry conditions. As shown by the authors, their relationship is highly sensitive to the averaging depth over which w_g is computed. The approaches of Dickinson (1984) and Wetzal and Chang (1987) prescribe a particular shape of the water profile close to the surface. The threshold method removes the problem of q_g and q_s specification.

3. Calibration of soil transfer coefficients against in situ data

In this section, the Montfavet data used to evaluate the behavior of the various parameterizations of bare soil evaporation are presented. Since very detailed measurements of the soil properties are available, a calibration of the soil-dependent coefficients in the NP89 scheme is performed.

a. Description of the Montfavet data

The experiment was performed during a one-week period (19–26 June 1984) at the location of Montfavet (France) to document within a $100 \times 100 \text{ m}^2$ plot the progressive drying of a bare soil after an irrigation period. The hydrodynamics and textural properties of the soil were determined accurately within the experimental domain. The water content profiles were measured every day by neutron access tubes at five locations (80-cm depth), together with hydraulic head profiles by tensiometers. The soil temperature profiles obtained by thermal probes (25-cm depth) were used to estimate the thermal conductivity. Soil samples were taken at different locations within the first 30 cm of soil to infer the mean dry bulk density, the textural components, and the saturated hydraulic conductivity. The textural analysis reveals that the soil type corresponds to the “silty clay loam” of the USDA textural classification. A micrometeorological station recorded the wind velocity, temperature, and vapor pressure at four levels in the air every 30 min. These profiles were used to obtain the sensible and latent heat fluxes by three classical methods (aerodynamic, Bowen ratio, energy balance). However, the results shown by Passerat (1986) show large differences between the methods used to estimate these fluxes. Therefore Passerat et al. (1989) derived daily accumulated evaporation values from soil water variations (i.e., water balance at the soil–atmosphere interface). The soil heat flux at the surface has been deduced from two methods: the aerodynamic method, where this quantity is inferred by balancing the surface energy budget, and the harmonic method consisting in a Fourier series decomposition of the near-surface soil temperature. The downward solar and atmospheric radiation fluxes were also measured.

b. Calibration of soil coefficients of the land surface scheme

Over bare soil, the NP89 scheme, derived from Blackadar (1976) and Deardorff (1977), predicts the evolution of four variables: the surface temperature T_s , the mean daily surface temperature T_2 , the surface volumetric water content within a thin soil layer (1 cm) w_g , and the mean volumetric water content w_2 . The equations for T_s and w_g include quantities which depend upon soil moisture and soil texture:

$$\frac{\partial T_s}{\partial t} = C_T G - \frac{2\pi}{\tau} (T_s - T_2) \quad (9)$$

$$\frac{\partial w_g}{\partial t} = \frac{C_1}{\rho_w d_1} (P_g - E_g) - \frac{C_2}{\tau} (w_g - w_{geq}), \quad (10)$$

where P_g is the flux of liquid water reaching the soil surface, G the soil heat flux, w_{geq} the equilibrium near-surface water content, ρ_w the density of liquid water, and $\tau = 1$ day.

Passerat et al. (1989) have shown that within a thin crust near the surface, textural properties depart significantly from those of the deep soil layers. As a consequence, an accurate calibration of the coefficients C_T and C_1 is necessary since they are related to the superficial moisture content.

If λ and c_g are the thermal conductivity and capacity of the soil, respectively, the coefficient C_T can be expressed by:

$$C_T = 2 \left(\frac{\pi}{\lambda c_g \tau} \right)^{1/2} \quad (11)$$

assuming a sinusoidally varying value of the ground heat flux G .

The dependence of the thermal conductivity λ on soil water w has been deduced from a relation proposed by Al Nakshabandi and Kohnke (1965) previously used by NP89:

$$\lambda = \max\{0.172, 418 \exp[-\log\psi(w) + 2.7]\}. \quad (12)$$

Measurements of the matrix potential as a function of soil moisture provide the relationship $\psi(w)$ as shown in Fig. 4 from Passerat et al. (1989). In Fig. 2, one can compare variations of λ with soil moisture derived from Eq. (12) against field and laboratory determinations. The agreement is good, although thermal conductivity appears to be overestimated when the soil is very moist.

If K is the hydraulic conductivity and $c_w = \partial w / \partial \psi$ the hydraulic capacity, the coefficient C_1 can be expressed by:

$$C_1 = 2 d_1 \left(\frac{\pi c_w}{K \tau} \right)^{1/2} \quad (13)$$

assuming a sinusoidal variation of the surface water flux.

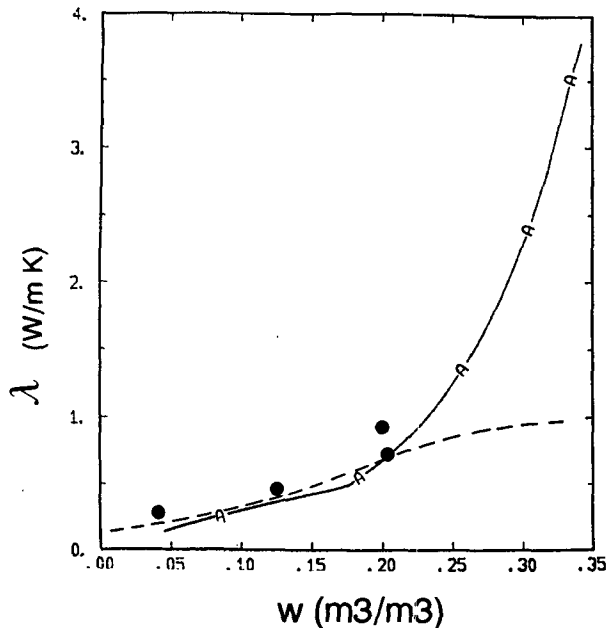


FIG. 2. Thermal conductivity as function of volumetric water content. Solid line: Eq. (12); dotted line: Passerat et al. (1989); full circles: laboratory measurements.

Experimental estimation of the curves $\psi(w)$ and $K(w)$ [the last one was fitted from an analytic expression proposed by Mualem (1976)] has allowed us to obtain variations of C_1 with soil water content in the surface layer (0.5 cm) (Fig. 3). This quantity appears to be almost constant except when the soil is very dry ($w \leq 0.15$). Therefore, the simulations to be presented afterwards will be performed with $C_1 = 0.3$. It is interesting to notice the importance of the knowledge of hydraulic properties, and to remark that when these latter are available from field data, the general formalism of NP89 is able to take such an information into account very easily. In the situation where the single information available is the soil type, the relationships $\psi(w)$ and $K(w)$ proposed by Clapp and Hornberger (1978) would have to be used. However the coefficient obtained in such a way is considerably higher than the one deduced from in situ hydraulic relations (Fig. 3).

For the coefficients C_2 and w_{geq} , which depend upon moisture in the deep soil, we have kept the calibration of NP89 using the Clapp and Hornberger (1978) classification for silty clay loam.

4. Model results

The simulations to be presented are run for seven days starting from 1100 LST 19 June 1984. The prognostic variables of the surface scheme have been initialized according to measurements within the soil both for moisture content and temperature ($w_g d_1 = 2.9$ mm; $w_2 d_2 = 240$ mm; $T_s = 22^\circ\text{C}$; $T_2 = 23^\circ\text{C}$). The total

soil depth is equal to 81 cm corresponding to the deeper level of measurement. The surface properties have been deduced from values of Passerat et al. (1989), but are kept constant during the simulations. The albedo is set to 0.2, the emissivity to 0.95, and the surface roughness to 1 mm (we assume that the roughness lengths for water vapor, sensible heat, and momentum are equal). Five parameterizations of E_g are tested according to Table 2.

Test 1 corresponds to the NP89 formulation. In order to avoid excessive dew flux over very dry soils, the surface water flux is set to zero except when $q_{sat}(T_s) \leq q_a$, in which case we set $\alpha = 1$ (see Table 2).

Test 2 refers to the β method with soil resistance R_{soil} calibrated by Passerat (1986) from a multilayer model.

Test 3 corresponds again to a β scheme. Like Dear-dorff (1978), we look for a simple expression of β from soil moisture in order to reduce the number of parameters to be specified. The soil resistance is highly variable with the soil type (see Fig. 4a) and Kondo et al. (1990) have shown that β is nearly independent of the aerodynamic resistance R_a (see Fig. 4b of Kondo et al. 1990). Figure 4b shows a plot of β variations versus the relative soil water content for different expressions of R_{soil} available in the literature. The moisture availability β has been computed for $R_a = 50 \text{ s m}^{-1}$ corresponding to the windy conditions during the last days of the observations (mean wind speed 7 m s^{-1}). Except for the Sun (1982) expression, β varies from 0 to 1,

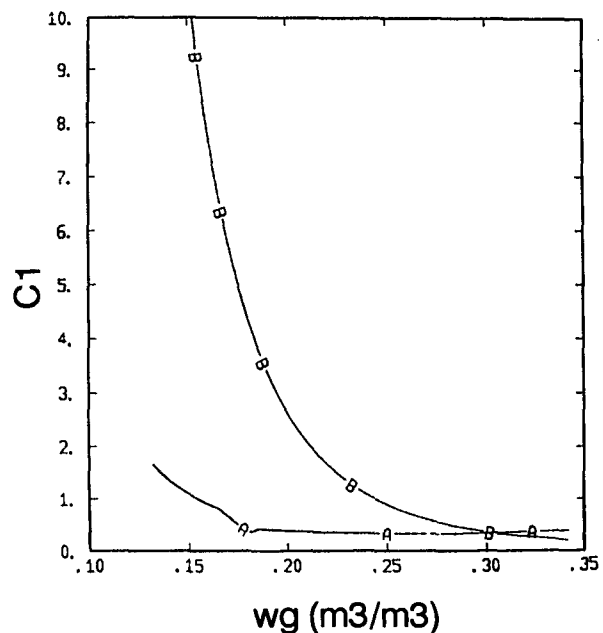


FIG. 3. Variations of the dimensionless coefficient C_1 vs volumetric water content according to Eqs. (19) and (20) from Noilhan and Planton (1989). Curve A: experimental hydraulic properties; curve B: hydraulic properties of Clapp and Hornberger (1978).

TABLE 2. Summary of evaporation formulation used in the five tests.

Test	Evaporation formulation
1	$E_g = \frac{\rho}{R_a} (q_g - q_a)$ <p>with $q_g = \max[\alpha q_{sat}(T_s), q_a]$ and $\alpha = \text{Eq. (NP89)}$ if $q_{sat}(T_s) \geq q_a$ with $q_g = q_{sat}(T_s)$ if $q_{sat}(T_s) < q_a$</p>
2	$E_g = \frac{\rho}{R_a + R_{soil}} [q_{sat}(T_s) - q_a]$ <p>with $R_{soil} = \text{Eq. (P86)}$</p>
3	$E_g = \frac{\rho}{R_a} \beta [q_{sat}(T_s) - q_a]$ <p>with $\beta = \text{Eq. (NP89)}$</p>
4	$E_g = \frac{\rho}{R_a + R_{soil}} [hq_{sat}(T_s) - q_a]$ <p>with $R_{soil} = \text{Eq. (P86)}$ and $h = \text{Eq. (1)}$</p>
5	$E_g = \min\left\{\rho_w E_t, \frac{\rho}{R_a} [q_{sat}(T_s) - q_a]\right\}$ <p>with $E_t = \text{Eq. (WC87)}$</p>

the maximum values being for a comparable value of soil moisture ($w_g \approx 0.60w_{sat}$). Figure 4b shows that $\beta = \alpha$ from NP89 fits this set of curves quite well.

Test 4 corresponds to the more complex β method

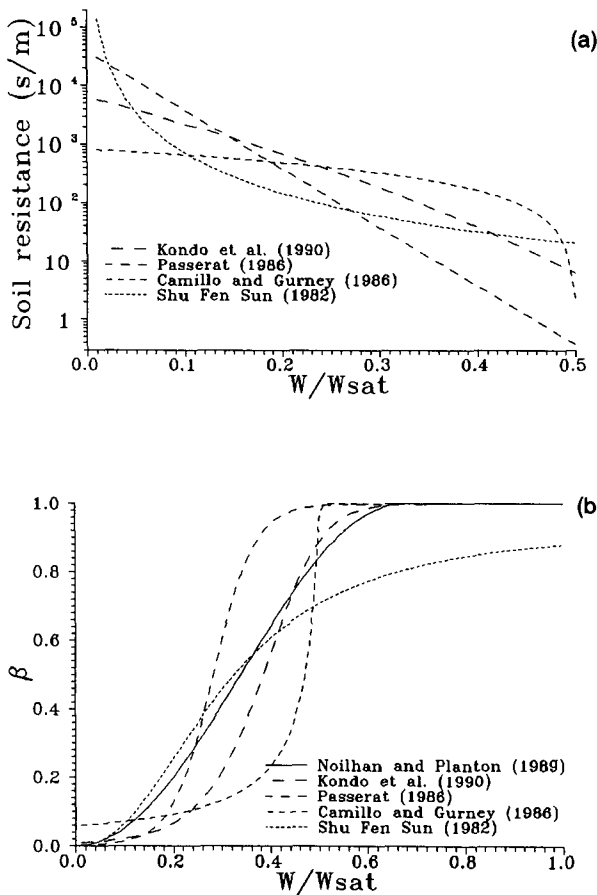


FIG. 4. Soil resistance (a) and moisture availability coefficient β (b) as function of relative water content (see Table 1). The coefficient β is computed for a value of $R_a = 50 \text{ s m}^{-1}$.

used by Dorman and Sellers (1989). This test is similar to test 2 except for the expression of q_s . The water potential in Eq. (1) is estimated from the Clapp and Hornberger (1978) relationship $\psi = \psi_{sat} (w/w_{sat})^{-b}$ for silty clay loam ($\psi_{sat} = -0.356 \text{ m}$, $w_{sat} = 0.477$, and $b = 7.75$).

Test 5 corresponds to the threshold evaporation formulation. In Fig. 5 are depicted the variations of E_t [Eqs. (MP84), (D84), (WC87), and (A88)] with surface moisture content w_g for silty clay loam and $w_2 = 0.3 \text{ m}^3 \text{ m}^{-3}$ which is the experimental value. Three of the curves behave similarly with E_t generally less than 100 W m^{-2} below $0.25 \text{ m}^3 \text{ m}^{-3}$, except in the formulation of Abramopoulos et al. (1988) where E_t has very high values above $0.25 \text{ m}^3 \text{ m}^{-3}$. Evaporation will first occur at a potential rate, rapidly reducing soil moisture. Since E_t decreases exponentially with soil moisture, this means that even with this threshold evaporation formulation the results should be similar to the other ones, in the context of this experiment. The formulation of Wetzel and Chang (1987) has been chosen because it is amenable to the structure of a simple two-layer model as they have claimed. According to Eq. (9) from Wetzel and Chang (1987), d has been set to $2d_1/C_1$ as derived by Noilhan and Planton (1989). This leads to a value of $d = 0.07 \text{ m}$.

We first examine the time evolution of both the near-surface water content and surface temperature (Fig. 6) and the cumulative evaporation (Fig. 7) during the seven experimental days.

Six experimental values of the volumetric water content obtained at 0.5 and 1.5 cm are reported in Fig. 6a. These measurements suggest that the vertical gradient of water increases with time as a result of the formation of a surface crust (see Passerat et al. 1989 for details). The predictions show a rapid decrease of w_g during the first three days followed by a period of quasi-steady behavior. At this stage, one can observe (except for test 5) very regular cycles where daily evaporation is compensated at night by capillary rises from

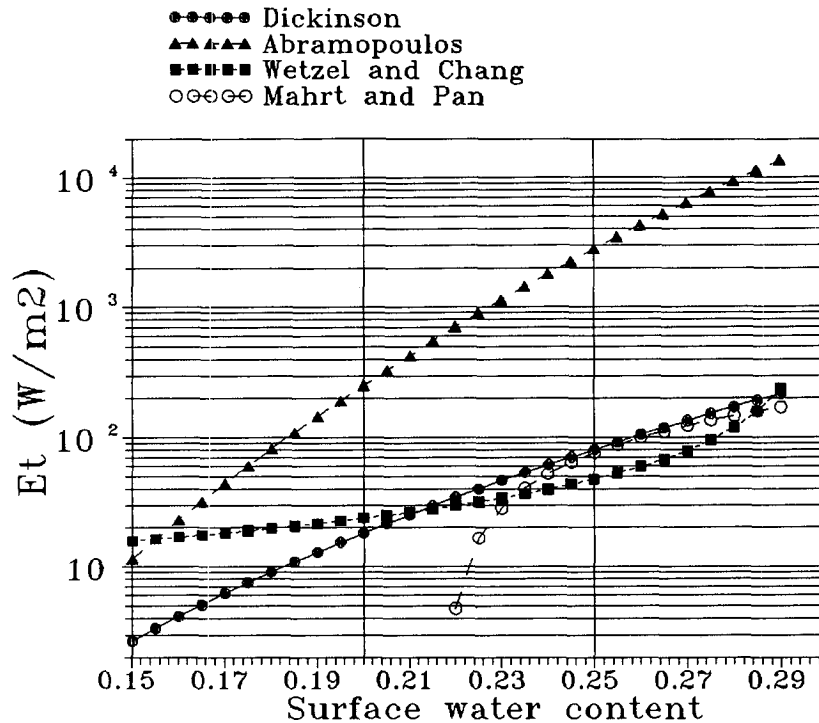


FIG. 5. Threshold evaporation as function of surface water content (see Table 1) for silty clay loam with $w_2 = 0.3 \text{ m}^3 \text{ m}^{-3}$, $d_1 = 1 \text{ cm}$, and $d = 7 \text{ cm}$.

the lower soil layer. The measurements show this continued drying of the soil surface as time progresses.

Test 1 predicts w_g variations in agreement with the observations at 1.5 cm. In tests 2, 3, and 4, the decrease of w_g in the two first days is more pronounced, particularly for test 2, the predictions lying between the experimental values at the two levels. One observes a stronger decrease of w_g in test 3 near 70 h of simulation due to the increase of the wind speed. Therefore, the expression for E_g in test 3 is more sensitive to the aerodynamic resistance than in the other β parameterizations. Because of the very low threshold value of E_t when w_g falls below $0.25 \text{ m}^3 \text{ m}^{-3}$ (Fig. 5), a very weak depletion of the surface reservoir is computed with test 5. As E_t is almost constant during the integration since it depends mainly on w_2 a stationary equilibrium is reached after day 2. A sensitivity test has shown that the evolution of w_g is strongly dependent upon the value of depth d . If one wishes to compute a depletion close to these observations one has to take a value of d about 1 mm, which seems to contradict the assumption of Wetzel and Chang (1987).

The predicted mean water content w_2 is nearly constant during the integrations as confirmed by observations of moisture in the lower layers.

Figure 6b gives the predictions for the surface temperature for tests 1–4. Results obtained from tests 2 and 3 are rather similar, with a reduction of the max-

imum of surface temperature near about 3 K with respect to tests 1 and 4 as a consequence of stronger evaporation (Fig. 7). Differences between tests 1 and 4 occur at night with higher values of surface temperature given by the NP89 formulation (test 1). The comparison of the predicted latent heat fluxes discussed afterward will help to understand these discrepancies.

Observed cumulative evaporation has been estimated in two ways (Fig. 7). In the first method, deduced from the surface energy balance and aerodynamic measurements, the amount of evaporation reaches 17.9 mm after six days. The second method corresponds to the soil water budget and gives a rather large scatter as shown in Fig. 7. The larger variation in the cumulative evaporation is observed in the first two days due to the irrigation heterogeneity at the beginning of the experiment. The amount of evaporation from the second method is $20.2 \pm 6.4 \text{ mm}$ for the whole period. Test 1 predictions fit the atmospheric estimates well. At the end of the integration, the cumulative evaporation is close to the soil water budget method. However, the model does not follow the distinct evaporation regimes emphasized by the budget method, namely strong evaporation at nearly the potential rate followed by a decline of E_g accompanying the surface drying. In test 5, evaporation takes place at an almost constant rate $E_t = 100 \text{ W m}^{-2}$ leading to a considerable underestimation of cumulative evapo-

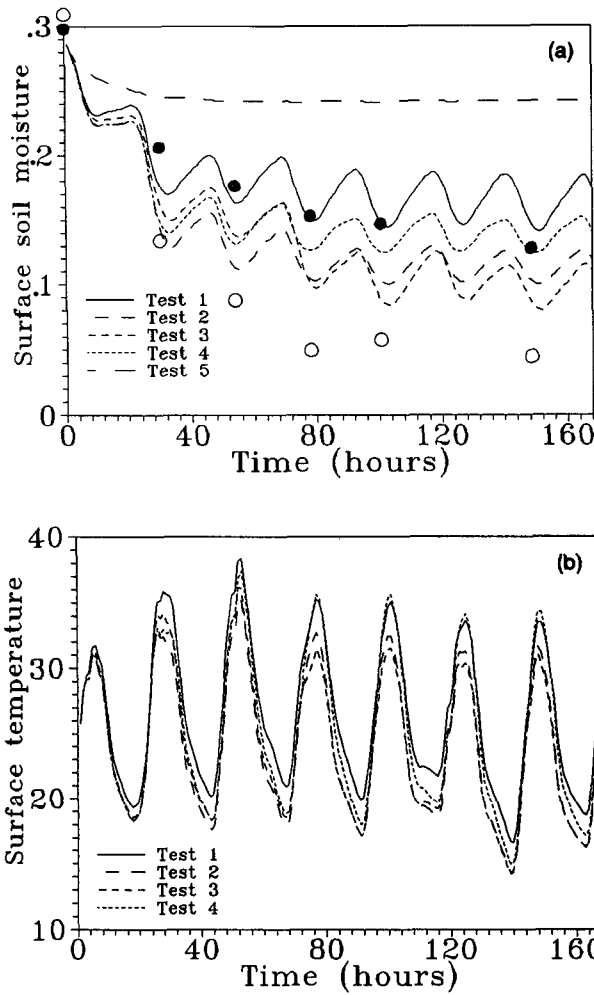


FIG. 6. Evolution of the surface moisture content (a) and of the surface temperature (b) during the seven days of simulation (from 1100 LST 19 June 1984 to 1100 LST 25 June 1984) for the sensitivity tests of Table 2. Daily observations of soil moisture are taken at 1.5 cm (full circles) and 0.5 cm (open circles).

ration. In these conditions, the threshold method totally suppresses the daily cycle of E_g . This conclusion is in agreement with the sensitivity study of Wetzell and Chang (1988) (see curve of Fig. 24 for the point scale). Such behavior may be understood by looking at the comparative evolution of the potential and threshold evaporations (Fig. 8). When $d = 4$ mm is chosen, a larger value of cumulative evaporation is computed (≈ 25 mm) as a consequence of a larger threshold value leading to quasi-potential evaporation at the beginning of the integration.

Tests 2 and 3 give quite similar results and clearly overestimate E_g as a consequence of the assumption $h = 1$. Without this hypothesis (test 4), an important reduction of the integrated evaporation of 3.5 mm is observed. It is difficult to evaluate accurately the dif-

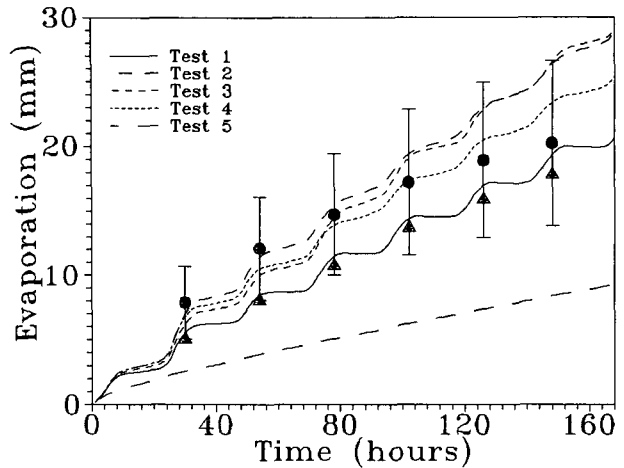


FIG. 7. As in Fig. 6 but for cumulative evaporation. Estimations are deduced from observed water budget (full circles with standard deviations) and aerodynamic measurements (full triangles).

ferences between tests 1 and 4 from these integrated quantities, and a detailed examination of the diurnal cycles of fluxes is required.

Figure 9 shows the observed and predicted variations of the soil heat flux G . Tests 1 and 4 give comparable predictions with high values of G for days 2 and 3 followed by a slow decrease of the maximum when the wind speed increases. The decrease of R_a up to day 4 leads to a strong increase of the sensible heat flux H . The two simulations are in fair agreement with estimates from the harmonic method. This method is based on measurement of soil temperature profiles and is very accurate. It gives lower values of G than the aerodynamic method, which seems to produce unrealistic values, especially on the second day around noon. This is a satisfactory result and gives credence

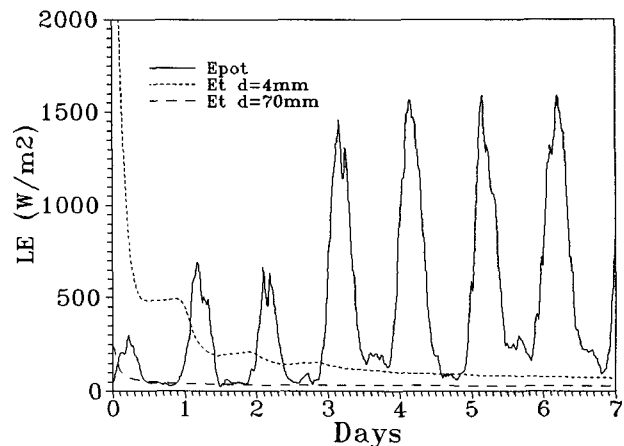


FIG. 8 Evolution of potential and threshold evaporations for test 5 and for two values of the depth d .

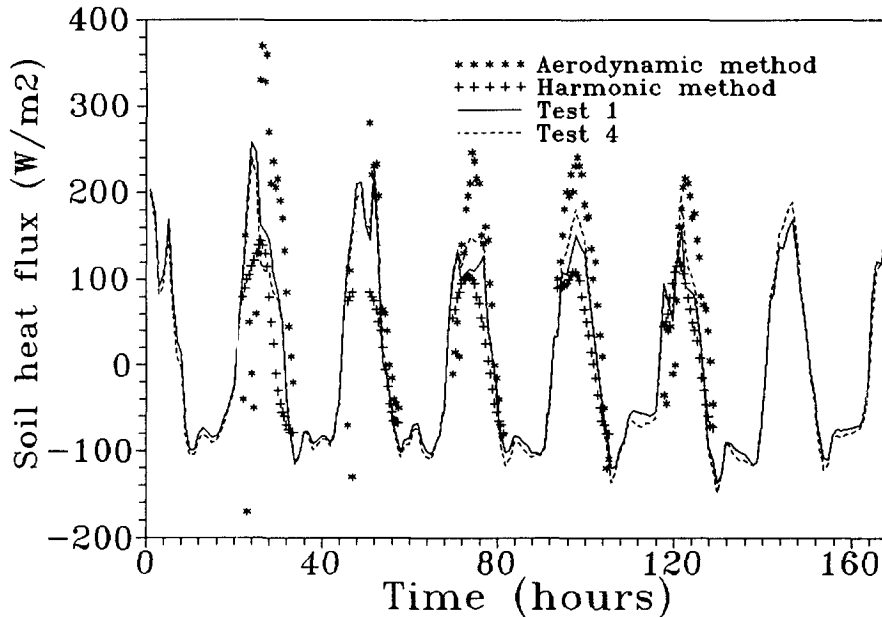


FIG. 9. Comparison between observed and predicted soil heat fluxes. Observations are only available during the daytime.

to the Blackadar (1976) force-restore method for the computation of surface temperature.

Figure 10 shows the predictions of LE_g (Fig. 10a) and H (Fig. 10b) for tests 1 and 4. The LE_g predictions during the day are not very different for the two tests, although the decrease of LE_g is obtained earlier in the afternoon for test 4. One also notes the high value of LE_g at noon for day 2 in test 4. This can be explained when looking at the evolution of h and α (Fig. 11). During the first two days, $h = 1$ and evaporation is potential. During the drying phase, the decrease of h is faster than that of α . The main discrepancy in LE_g predictions is observed at night. Indeed, test 4 predicts nocturnal evaporation close to 50 W m^{-2} while test 1 computes a negligible value. All the previous tendencies are reversed for the evolution of sensible heat flux (Fig. 10b).

The last comparison between model results and data presented in Fig. 12 shows two diurnal cycles of evaporation. Although the two experimental methods give rather scattered estimates during the day, they both show small values of LE_g at night, with some small dew formation before dawn. Test 1 predicts this nocturnal behavior more realistically than test 4. The nocturnal evaporation produced in test 4 leads to an enhanced cooling of the surface as noticed in Fig. 6b.

5. Concluding remarks

Various formulations of surface evaporation currently used in land surface parameterizations have been tested against detailed measurements of water and en-

ergy exchanges over loamy bare ground (Passerat et al. 1989). We have examined two main expressions, that is, classical bulk aerodynamic and threshold formulations, which relate the evaporation flux to the near-surface water content and to the soil properties. The tests have been conducted with a land surface scheme (Noilhan and Planton 1989) constrained to follow the observed atmospheric forcing at the reference level during one week. Due to the modeling method, differences between the various tests are enhanced to some extent because no feedback has been allowed between the atmosphere and the surface processes. Since measurements were taken just after irrigation, a significant decrease of superficial moisture was observed (from field capacity to wilting point) in response to the clear sky conditions prevailing during the experimental period. Model results have been mainly compared with observed variations of daily estimates of superficial water content and cumulative evaporation.

The bulk aerodynamic formulations provide comparable results during the daytime. On the other hand, the β methods seem to overestimate the nocturnal evaporation. Discrepancies in nighttime predictions involve differences of cumulative evaporation of about 20% between the α and β methods. Consequently, a better knowledge of nocturnal evaporation is needed with accurate measurements of the dew flux. The α method (test 1) requires a specific treatment of dew in order to prevent excessive values over very dry soils, whereas the β method (test 4) necessitates prior calibration of the soil resistance with soil moisture for different soil textures. An alternative way may consist in

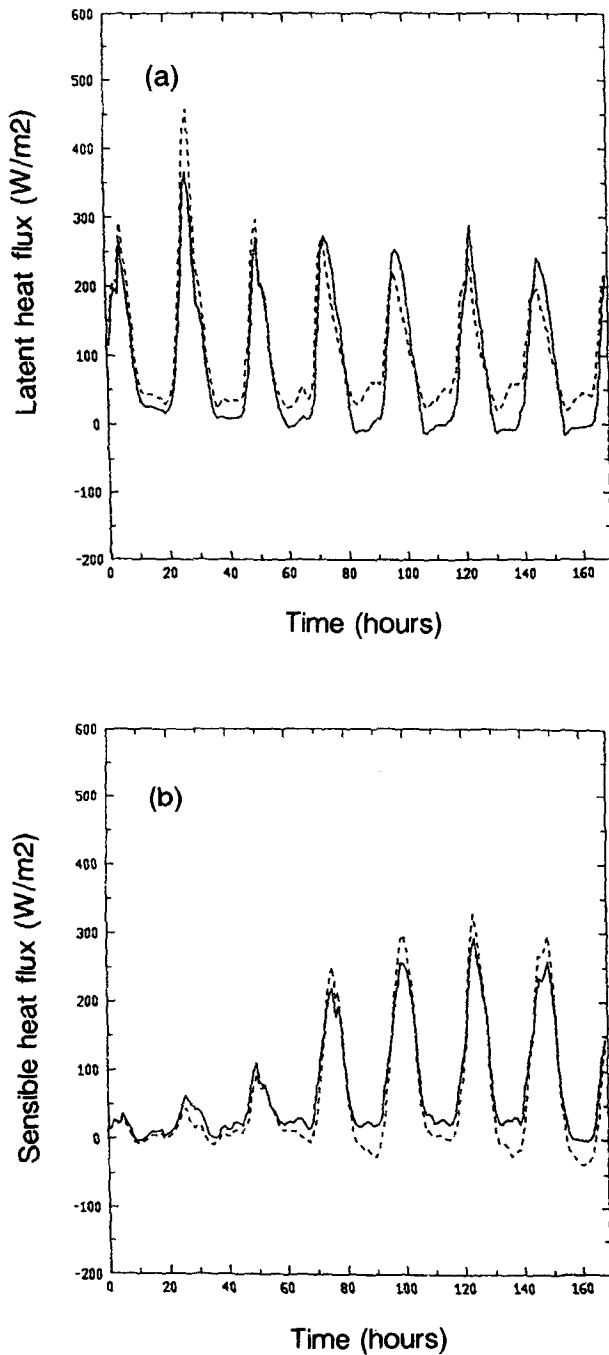


FIG. 10. Comparison of predicted latent heat flux (a) and sensible heat flux (b) between test 1 (solid line) and test 4 (dotted line).

using a simple relationship between β and soil moisture (test 3).

Threshold formulations appear to be very sensitive to the specification of the depth over which the diurnal cycle of moisture is damped. In the context of this dataset, threshold methods strongly underestimate evap-

oration (test 5). Moreover, they cannot predict a diurnal cycle for evaporation and a drastic transition occurs from potential to limited supply regimes. Threshold methods are also more sensitive to the general enhancement of potential evaporation due to the overestimation of surface temperature computed from a dry surface energy balance (Mahrt and Ek 1984).

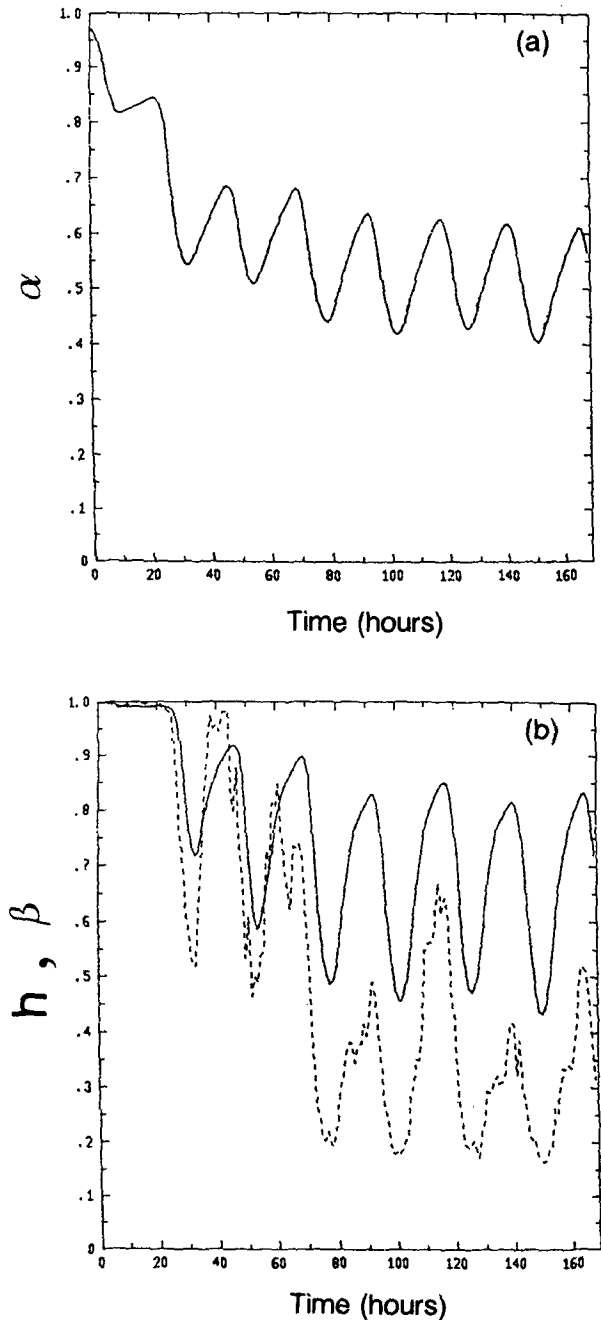


FIG. 11. Time evolution of α (a) in test 1, h (solid line) and β (dotted line) (b) in test 4.

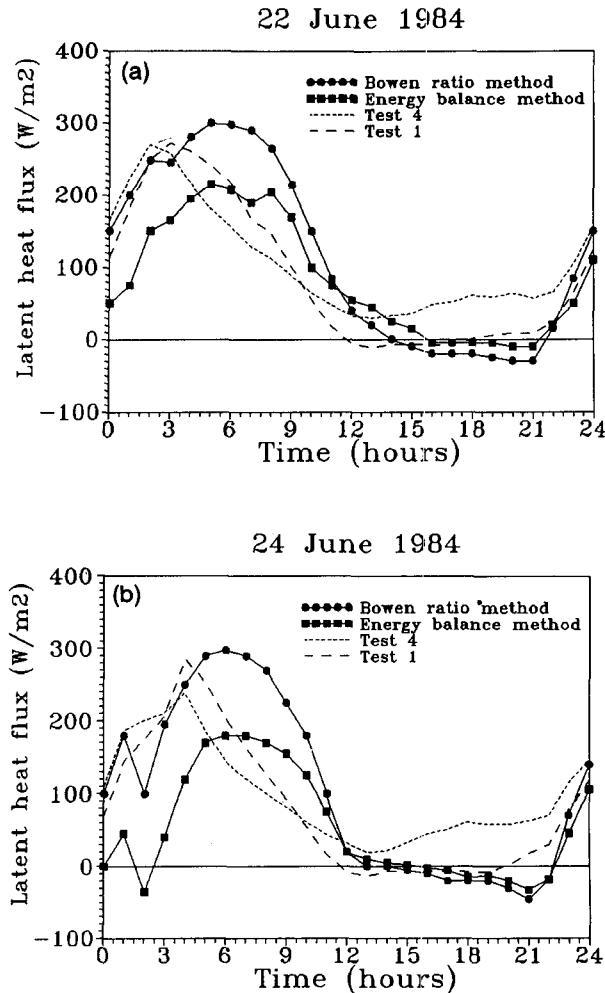


FIG. 12. Comparison between observed and predicted latent heat fluxes on 22 June (a) and 24 June 1984 (b).

This dataset has allowed us to further validate our surface scheme over bare ground. Of particular interest is the encouraging prediction of the ground heat flux since this quantity represents a major component of the surface energy balance over bare ground.

This study outlines the great interest in collecting long enough time series of in situ data to perform intercomparisons of land surface parameterizations prior to their implementation in meteorological models. We plan similar studies over vegetated areas taking advantage of the ARME (Shuttleworth et al. 1984), HAPEX (André et al. 1986), and FIFE (Sellers et al. 1988) experiments.

Acknowledgments. We thank very much M. Vauclin for providing us with the data and M. J. Germain for assistance with the data processing. We have greatly benefited from helpful comments and suggestions from P. Mascart, S. Planton, and M. Vauclin. Our gratitude

also goes to Ph. Bougeault for his encouragement during this study. V. Balaji and R. Benoit carefully reviewed the manuscript.

REFERENCES

- Abramopoulos, F., C. Rosenzweig and B. Choudhury, 1988: Improved ground hydrology calculations for global climate models (GCMs): Soil water movement and evapotranspiration. *J. Climate*, **1**, 921-941.
- Al Nakshabandi, G., and H. Konhke, 1965: Thermal conductivity and diffusivity of soils as related to moisture tension and other physical properties. *Agric. Meteorol.*, **2**, 271-279.
- André, J. C., J. P. Goutorbe and A. Perrier, 1986: HAPEX-MOBILHY: A hydrologic atmospheric experiment for the study of water budget and evaporation flux at the climatic scale. *Bull. Amer. Meteor. Soc.*, **67**, 138-144.
- Barton, I. J., 1979: A parameterization of the evaporation from non-saturated surfaces. *J. Appl. Meteorol.*, **18**, 43-47.
- Blackadar, A. K., 1976: Modeling the nocturnal boundary layer. *Proc. of the Third Symp. on Atmospheric Turbulence, Diffusion, and Air Quality*. Amer. Meteor. Soc., 46-49.
- Brunet, Y., 1984: Modélisation des échanges sol nu-atmosphère. Essai de validation locale et influence de la variabilité spatiale du sol. thesis, Université Scientifique et Médicale de Grenoble.
- Brutsaert, W. H., 1982: *Evaporation into the Atmosphere*. D. Reidel Publishing Company, 299 pp.
- Camillo, P. J., and R. J. Gurney, 1986: A resistance parameter for bare soil evaporation models. *Soil Science*, **141**, 95-105.
- , —, and T. J. Schmugge, 1983: A soil and atmospheric boundary layer for evapotranspiration and soil moisture studies. *Water Resour. Res.*, **19**, 371-380.
- Choudhury, B. J., and J. L. Monteith, 1988: A four-layer model for heat budget of homogeneous land surfaces. *Quart. J. Roy. Meteor. Soc.*, **114**, 373-398.
- Clapp, R. B., and G. M. Hornberger, 1978: Empirical equations for some hydraulic properties. *Water Resour. Res.*, **14**, 601-604.
- Deardorff, J. W., 1977: A parameterization of the ground surface moisture content for use in atmospheric predictions models. *J. Appl. Meteorol.*, **16**, 1182-1185.
- , 1978: Efficient prediction of ground temperature and moisture with inclusion of a layer of vegetation. *J. Geophys. Res.*, **83**, 1889-1903.
- Dickinson, R. E., 1984: Modeling evapotranspiration for three-dimensional global climate models. *Climate Processes and Climate Sensitivity*, Amer. Geophys. Union, Geophys. Monogr., 58-72.
- Dorman, J. L., and P. J. Sellers, 1989: A global climatology for albedo, roughness length, and stomatal resistance for atmospheric general circulation models as represented by the Simple Biosphere model (SiB). *J. Appl. Meteorol.*, **28**, 833-855.
- Germain, M. J., 1990: Validation d'une paramétrisation des échanges de surface sur différents types de végétation. Tech. Rep. E. N. M., [Available from CNRM, 42, Avenue Coriolis, 31057 Toulouse cedex, France].
- Jacquemin, B., and J. Noilhan, 1990: Sensitivity study and validation of a land surface parameterization using the HAPEX-MOBILHY dataset. *Bound.-Layer Meteorol.*, **52**, 93-134.
- Kondo, J., N. Saigusa and T. Sato, 1990: A parameterization of evaporation from bare soil surfaces. *J. Appl. Meteorol.*, **29**, 385-389.
- Louis, J. F., M. Tiedke and J. F. Geleyn, 1981: A short history of the operational PBL parameterization of the ECMWF. *Workshop on Planetary Boundary Layer*, ECMWF, 59-79.
- Mahfouf, J. F., 1986: Contribution à la définition d'une paramétrisation des transferts entre le sol, la végétation, et l'atmosphère. Analyse de sensibilité et insertion dans un modèle de méso-échelle. thesis, Université de Clermont II.
- , 1990: A numerical simulation of the surface water budget during HAPEX-MOBILHY. *Bound.-Layer Meteorol.*, **53**, 201-222.

- , and B. Jacquemin, 1989: A study of rainfall interception using a land surface parameterization for mesoscale meteorological models. *J. Appl. Meteor.*, **28**, 1282–1302.
- Mahrt, L., and M. Ek, 1984: The influence of atmospheric stability on potential evaporation. *J. Climate Appl. Meteor.*, **23**, 222–234.
- , and H. Pan, 1984: A two-layer model of soil hydrology. *Bound-Layer Meteor.*, **29**, 1–20.
- McCumber, M. C., and R. A. Pielke, 1981: Simulation of the effects of surface fluxes of heat and moisture in a mesoscale numerical model. Part I: Soil layer. *J. Geophys. Res.*, **86**, 9929–9938.
- Mualem, Y., 1976: A new model for predicting the hydraulic conductivity of unsaturated porous media. *Water Resour. Res.*, **12**, 513–521.
- Nappo, C. J., 1975: Parameterization of surface moisture and evaporation rate in a planetary boundary layer model. *J. Appl. Meteor.*, **14**, 289–296.
- Noilhan, J., 1987: Une modélisation unidimensionnelle des transferts énergétiques dans le sol, la végétation et la couche limite atmosphérique. Tech. Rep. 171, EERM, [Available from CNRM, 42, Avenue Coriolis, 31057 Toulouse cedex, France].
- , and S. Planton, 1989: A simple parameterization of land surface processes for meteorological models. *Mon. Wea. Rev.*, **117**, 536–549.
- Passerat de Silans, A., 1986: Transferts de masse et de chaleur dans un sol stratifié soumis à une excitation atmosphérique naturelle. Comparaison: Modèles-expérience. thesis, Institut National Polytechnique de Grenoble.
- , L. Bruckler, J. L. Thony and M. Vauclin, 1989: Numerical modeling of coupled heat and water flows during drying in a stratified bare soil-comparison with field observations. *J. Hydrol.*, **105**, 109–138.
- Philip, J. R., 1957: Evaporation and moisture and heat field in the soil. *J. Meteor.*, **14**, 354–366.
- Sasamori, T., 1970: A numerical study of atmospheric and soil boundary layers. *J. Atmos. Sci.*, **27**, 1122–1137.
- Sellers, P. J., F. G. Hall, G. Asrar, D. E. Strebel and R. E. Murphy, 1988: The First ISLSCP Field Experiment (FIFE). *Bull. Amer. Meteor. Soc.*, **69**, 22–27.
- Shuttleworth, J., and collaborators, 1984: Eddy correlation of energy partition for Amazonian forest. *Quart. J. Roy. Meteor. Soc.*, **110**, 1143–1162.
- Sun, Shu Fen, 1982: Moisture and heat transport in a soil layer forced by atmospheric conditions. M.S. thesis, University of Connecticut.
- Wetzel, P. J., and J. T. Chang, 1987: Concerning the relationship between evapotranspiration and soil moisture. *J. Climate Appl. Meteor.*, **26**, 18–27.
- , and —, 1988: Evapotranspiration from nonuniform surfaces: a first approach for short term numerical weather prediction. *Mon. Wea. Rev.*, **116**, 600–621.
- Yasuda, N., and T. Toya, 1981: Evaporation from nonsaturated surface and surface moisture availability. *Pap. Meteor. Geophys.*, **32**, 89–98.